International Journal of Climatology

Do global warming-induced circulation pattern changes affect temperature and precipitation over Europe during summer?

Alexandre Belleflamme, Xavier Fettweis, Michel Erpicum

Affiliations and address:

A. Belleflamme

Laboratory of Climatology and Topoclimatology

University of Liège

Allée du 6 Août, 2, 4000 Liège, Belgium

Tel.: +32-43-665354

Fax: +32-43-665722

A.Belleflamme@ulg.ac.be

X. Fettweis and M. Erpicum

Laboratory of Climatology and Topoclimatology, University of Liège, Belgium

Abstract

Future climate change projections are not limited to a simple warming, but changes in precipitation and sea level pressure are also projected. The sea level pressure changes and the associated atmospheric circulation changes could directly mitigate or enhance potential projected changes in temperature and precipitation associated to rising temperatures. With the aim of analysing the projected circulation changes and their possible impacts on temperature and precipitation over Europe in summer (JJA), we apply an automatic circulation type classification method, based on daily sea level pressure, on general circulation model (GCM) outputs from the CMIP5 data base over the historical period (1951-2005) and for climate under two future scenarios (2006-2100). We focus on summer as it is the season when changes in temperature and precipitation have the highest impact on human health and agriculture. Over the historical observed reference period (1960-1999), our results show that most of the GCMs have significant biases over Europe when compared to reanalysis datasets, both for simulating the observed circulation types and their frequencies, as well as for reproducing the intraclass means of the studied variables. The future projections suggest a decrease of circulation types favouring a low centred over the British Isles for the benefit of more anticyclonic conditions. These circulation changes mitigate the projected precipitation increase over north-western Europe in summer, but they do not significantly affect the projected temperature increase and the precipitation decrease over the Mediterranean region and eastern Europe. However, the circulation changes and the associated precipitation changes are tarnished by a high uncertainty among the GCM projections.

Keywords

General Circulation Models, Sea level pressure, Europe, Circulation Type Classification,

Atmospheric circulation, Precipitation, Temperature

1. Introduction

As stated in the Intergovernmental Panel on Climate Change Fourth Assessment Report (IPCC AR4) (Meehl *et al.*, 2007), global warming is expected to induce a temperature increase over the next decades over Europe. Furthermore, summer (June, July, and August) precipitation is projected to decrease over southern Europe and increase over the northern part of the continent (Christensen *et al.*, 2007). Projections also suggest a decrease of the mean sea level pressure, particularly over the Mediterranean region in summer (Meehl *et al.*, 2007). These projected sea level pressure (SLP) changes lead to two questions. First, do the SLP changes induce atmospheric circulation changes, and if so, what kind of changes? Secondly, how do these circulation changes impact other variables such as near-surface temperature (TAS) and precipitation (PR)? This question is particularly crucial, as the circulation changes can either mitigate or enhance the direct changes of these variables induced by the temperature increase. This could also have an impact on extreme events, such as droughts, heavy rain events or heat waves as shown by Meehl and Tebaldi (2004) and Rowell and Jones (2006). However, the uncertainties concerning the impact of circulation changes on the precipitation regime are very high (Rowell and Jones, 2006).

A circulation type classification (CTC) is one of the ideal tools to study the relationship between the atmospheric circulation and near-surface climate variables, and their possible future changes. CTCs allow a precise study of the atmospheric circulation by grouping similar circulation situations together (Bardossy *et al.*, 2002 ; Philipp *et al.*, 2010). In addition, they are interesting tools for evaluating the ability of General Circulation Models (GCMs) to

reproduce the observed circulation (Anagnostopoulou *et al.*, 2008 ; Anagnostopoulou *et al.*, 2009 ; Belleflamme *et al.*, 2013 ; Demuzere *et al.*, 2009 ; Huth, 2000 ; Pastor and Casado, 2012) and for detecting changes in the atmospheric circulation (Bardossy and Caspary, 1990 ; Huth *et al.*, 2008 ; Fettweis *et al.*, 2013 ; Kyselý and Huth, 2006). Finally, many studies have shown that there is a strong link between atmospheric circulation types derived from CTCs and ground variables such as TAS and PR (Anagnostopoulou *et al.*, 2009 ; Bardossy *et al.*, 2002 ; Kyselý and Huth, 2006 ; Pasini and Langone, 2012).

With the aim of studying future circulation changes over Europe and their impact on PR and TAS, we use here the CTC developed by Fettweis *et al.* (2011) that we apply over Europe to outputs from 14 GCMs from the World Climate Research Programme (WCRP) Coupled Model Intercomparison Project phase 5 (CMIP5) multimodel dataset, which are compared with two reanalysis datasets over 1960-1999. We focus on summer (June, July, August [JJA]) since this is the season when the changes in TAS and PR are assumed to have the most important impacts on human health and agriculture. The data used are presented in Section 2. The CTC methodology is described in Section 3. Section 4 presents the results in two parts. First, we evaluate the ability of the GCMs to reproduce the historical observed atmospheric circulation in summer. Secondly, we analyse the circulation changes projected under global warming conditions and the impact of these changes on PR, TAS, and SLP.

2. Data

We here study the ability of 14 CMIP5 GCMs (listed in Table 1) to reproduce observed atmospheric circulation variability and climate in summer as well as analyse projected future circulation and climate changes. Simulations of daily mean SLP, TAS, and PR are analysed

for a 55-year historical period (1951-2005) summer (JJA) and future summers (2006-2100). For the future projections, we use the most common Representative Concentration Pathway (RCP) experiments: RCP4.5 (lower-end) and RCP8.5 (higher-end) projecting a radiative forcing of 4.5 W/m² and 8.5 W/m² at 2100, respectively (Moss *et al.*, 2010). These GCM outputs are compared with two reanalysis datasets over the period 1960-1999: the ERA-40 Reanalysis from the European Centre for Medium-Range Weather Forecasts (ECMWF) (Uppala *et al.*, 2005), and the NCEP/NCAR Reanalysis from the National Centers for Environmental Prediction - National Center for Atmospheric Research (Kalnay *et al.*, 1996). Since the spatial resolution differs from one dataset to the other (see Table 1), all the data were linearly interpolated on a regular grid of 3000 km x 2500 km covering the majority of Europe (see Fig. 1) at a spatial resolution of 100 km.

3. Methodology

The method used here is the automatic CTC developed by Fettweis *et al.* (2011) over the Greenland ice sheet. This classification is considered a leader-algorithm method (Philipp *et al.*, 2010). This means that for the first class, the day which counts the most similar days (on the basis of a similarity index, see below), is selected as the reference day (leader) (Fettweis *et al.*, 2011 ; Belleflamme *et al.*, 2013). All days, which are similar to it are grouped into this class and removed from the dataset. This procedure is repeated until all days are classified. As done by Belleflamme *et al.* (2013), we here used the Spearman rank correlation to evaluate the similarity between two daily circulation situations on the basis of the daily mean SLP. The Spearman rank correlation coefficient offers the advantage to take only the SLP pattern into account, regardless of changes in the mean SLP due to global warming. However, this is also a drawback, since this index does not take into account the gradient strength (Philipp *et al.*,

2007), which could impact the weather conditions on the surface. For example, a day presenting a weak anticyclone and another day characterized by a strong anticyclone could be grouped into the same class.

Since this classification is objective and automatic, meaning that the types are built by the algorithm and not predefined by the user, the circulation types are different for each dataset, making it difficult to do an easy intercomparison. As proposed by Huth (2000) and Huth *et al.* (2008), and already applied for this classification method over Greenland by Belleflamme *et al.* (2013), we project the classes of our reference dataset (ERA-40) onto the other datasets (GCMs), i.e. we apply the parameters defining the classes from the reference dataset to the other datasets. Thus, the classification results of all datasets are directly comparable class by class on the basis of their frequency differences. In this study, we used ERA-40 over 1960-1999 as the reference dataset, but the results are similar by using NCEP/NCAR as reference. For more details about the approach used in this paper, we refer to Belleflamme *et al.* (2013).

As said above, we use the SLP as the predictor variable and the intraclass TAS and PR means (i.e. means computed over all JJA days included in a given class) are computed when the SLP based classification has been performed. The number of classes, which is chosen by the user in this classification, is fixed to three here. The interest of using a very low number of classes (i.e. circulation types) is to represent the atmospheric circulation only through its most fundamental types; thereby the results are not impacted by the difficulty of GCMs to reproduce the less common circulation types, which could distort the analysis of the future changes of these types.

In order to synthesize our results in a few number of graphics, we have built scatter plots

(Figs. 2, 6, 7, and 8) as follows. For each circulation type, the GCM based JJA means of the anomalies of SLP, TAS, and PR are represented as a function of the JJA mean anomaly of TAS. Anomalies are computed with respect to the reference period (1960-1999) and are smoothed by a 10-year running mean in order to remove the interannual variability, which constitutes noise when calculating the relationship between the considered variables and TAS. We hereby obtain graphs of the projected evolution of each variables anomaly with increasing JJA temperature over Europe. The domain is split into quarters (NW, NE, SW, and SE, see Fig. 1), to allow a more precise spatial analysis of the projected intraclass changes of the different variables. For the frequency of circulation types, annual raw values (still smoothed by a 10-year running mean) are used instead of anomalies.

4. Results

The three circulation types derived from the SLP classification process for ERA-40 over 1960-1999 (JJA) can be described as follows: Type 1 is under the influence of an anticyclone situated to the north of the Azores islands which induces a north-westerly flow over Europe. This leads to colder than normal conditions over the major part of the domain, drier conditions over western Europe and wetter weather over eastern Europe. Type 2 is dominated by a low north of the British Isles leading to south-westerly flow and warmer and drier conditions over southern and eastern Europe contrasted by wetter and colder conditions in the north-western part of the domain. Type 3 has a very weak pressure gradient consisting of a mild low pressure over the Mediterranean region leading to lower temperatures and more precipitation in this area. The northern half of the domain experiences warmer and drier conditions for this circulation type than the 1960-1999 JJA average. These three circulation patterns are shown in Fig. 1.

4.1 Historical reference climate

Analysis of the root mean square error (RMSE) calculated by comparing the circulation type frequencies derived from ERA-40 reanalysis with each of the 14 GCMs over the historical reference period (1960-1999) shows significant discrepancies between the GCMs (see Table 2). Nevertheless, no systematic circulation type frequency bias through all the GCMs can be observed. For example, there is a strong improvement between the low resolution IPSL-CM5A-LR and the medium resolution IPSL-CM5A-MR, but there is no improvement between MPI-ESM-LR and MPI-ESM-MR. The analysis of the circulation type frequency biases between each GCM and ERA-40 for the reference period (1960-1999) shows that types 1 and 2 are generally underestimated (respectively by 9/14 and 10/14 GCMs), leading to an overestimation by 11/14 GCMs of Type 3, since this type contains the unclassified days (Belleflamme *et al.*, 2013) (see Table 2).

Further examination of the GCM biases for the three variables studied here (SLP, TAS, and PR) in each quarter of the domain shows that biases related to PR intraclass anomalies appear to be systematic. Fig. 2 shows that the PR anomalies from all the GCMs are generally not contrasted enough (i.e. the dryer regions of a given type are too wet, and the wetter regions are too dry) with regard to ERA-40 over 1960-1999 (see also circles on Fig. H in the Supplementary Material). This underestimation of the PR intraclass anomalies might be related to the generalised GCM underestimation of the precipitation amount (PR intraclass mean) over northern and eastern Europe, while some of them overestimate the PR amount over the Iberian peninsula and parts of the Mediterranean basin (see Fig. 3).

The TAS anomalies are much better reproduced, despite there is a too low anomaly for Type 1

for most GCMs over most subdomains (see circles on Fig. G in the Supplementary Material). There is no link with the TAS intraclass mean biases, which are very different from one GCM to another. In general, the biases are consistent over all subdomains and all circulation types of a given GCM. For example, BNU-ESM systematically overestimates TAS, while BCC-CSM1-1, MPI-ESM-LR, MPI-ESM-MR, and MRI-CGCM3 underestimate TAS. This spread of the GCM biases is confirmed by the JJA bias over 1960-1999 (see Fig. 4), which is very different from one GCM to another.

Contrary to the TAS anomaly, the Type 1 SLP anomaly is generally overestimated for the four subdomains by GCMs (see circles on Fig. F in the Supplementary Material). No systematic biases are detected for the other types. However, some exceptions need to be pointed out (see Fig. 5): CanESM2 overestimates the Type 1 SLP intraclass mean only over the NW quarter, BCC-CSM1-1 underestimates it over the NE quarter, CNRM-CM5 shows different biases depending on the subdomains and the types, and both MPI-ESM-LR and MPI-ESM-MR underestimate the SLP mean over the northern half of the domain. Furthermore, the mean pattern (shown by the black isobars on Fig. 5) is very different for some GCMs (e.g. CNRM-CM5, GFDL-ESM2M, and MRI-CGCM3) with regard to the ERA-40 pattern.

4.2 Future climate

In this section, we focus on the RCP8.5 experiment (for the corresponding RCP4.5 figures, see Supplementary Material). This is justified, since there is no major difference in the relationship between the circulation type frequency, SLP, TAS, and PR on one side, and TAS on the other side when using RCP4.5 instead of RCP8.5. The only difference is a stronger warming in RCP8.5 and consequently stronger changes in circulation type frequency, SLP, TAS, and PR.

The analysis of each GCM separately reveals that the biases related to intraclass anomalies over the historical period strongly impact the future projected intraclass anomalies. As it appears on the scatter plots of each GCM (see Supplementary Material Figs. E to L), the relationship between circulation type frequency, SLP, TAS, and PR and the seasonal mean temperature is linear. Furthermore, the future projection experiments are in the continuity of the historical experiment, so that the biases of the historical period remain in the future projections.

4.2.1 Frequency of circulation types

Most of the GCMs suggest a decrease in frequency of Type 2 with rising temperatures (see Fig. 6 ; see also Fig. A in the Supplementary Material for RCP4.5). This decrease is compensated by a frequency increase of Type 1 and to a lesser extent of Type 3. This finding is in agreement with the general decrease of SLP projected by most of the GCMs over the Mediterranean region, as depicted by the colour shading in Fig. 5. Nevertheless, the decrease amount in frequency of Type 2 differs from one GCM to another (see Figs. E and I in the Supplementary Material for RCP4.5 and RCP8.5 respectively). In general, we can say that the more a GCM overestimates (resp. underestimates) the frequency of Type 2, the stronger (slighter) is the decrease. The average regression slope of the five GCMs overestimating the Type 2 frequency is of -4.42 ± 1.26 %/year, while the nine GCMs underestimating the Type 2 frequency have an average slope of -1.54 ± 0.98 %/year. An analogue analysis can be done for the Type 1 frequency increase. The seven GCMs, that underestimate the frequency of Type 1, show an average slope (2.65 ± 0.98 %/year), which is higher than the average slope of the underestimating GCMs (1.21 ± 0.46 %/year). Obviously, the circulation type frequency biases over the historical period do not only impact the offset of the projected changes, they also

influence the strength of the changes. Finally, the changes in frequency of Type 3 are not as clear. Seven GCMs project a Type 3 frequency decrease (CNRM-CM5, IPSL-CM5A-LR, and MRI-CGCM3) or nearly no change (GFDL-ESM2M, IPSL-CM5A-MR, MIROC-ESM-CHEM, and MIROC-ESM), while the remaining seven GCMs project an increase in frequency.

4.2.2 Sea Level Pressure

Nine of our selected GCMs project a decrease in SLP for the future, suggesting a link between global warming and an SLP decrease over Europe in summer. Four of the remaining GCMs (BCC-CSM1-1, CNRM-CM5, MPI-ESM-LR, and MPI-ESM-MR) do not project a significant change in SLP, while GFDL-ESM2M simulates rather an increase towards 2100 (see also Fig. 5, where it appears that MPI-ESM-LR, MPI-ESM-MR, and to a lesser extend BCC-CSM1-1 project an increase in SLP over the northern half of the domain). This figure also gives an idea of the range of the projected SLP change among the 14 GCMs. It is important to note that, for most GCMs, the magnitude of the projected SLP change is of the same order of magnitude as the SLP bias over the historical period with regard to ERA-40. Nevertheless, except BCC-CSM1-1, the GCMs projecting no change or an increase in SLP are the least successful at reproducing the reference period circulation over Europe in summer (see Table 2).

When further analysing the regional differences in the projected SLP change, we can see that a slight increase of SLP is projected over the north-western part of the domain (see Fig. 5). Therefore, the slight reinforcement of the east-west gradient logically favours circulation Type 1, as opposed to Type 2, which presents a pattern opposed to the projected decrease of SLP over the southern part of the domain. Nevertheless, the intraclass change of the SLP anomaly with increasing TAS shows for the NW quarter a significant decrease for all types (see Fig. 7 ;

see also Fig. B in the Supplementary Material for RCP4.5), which seems to be in contradiction with the slight mean SLP increase described before. But, despite there is an SLP decrease in each type, the frequency of Type 1 (showing a higher SLP than the other types in NW) is projected to increase to the detriment of Type 2 (showing the most negative SLP anomaly).

In order to highlight the influence of the circulation changes on the SLP, TAS, and PR changes, we have computed the "no circulation" change, which takes only the intraclass changes into account (see Table 3). For each GCM, the "no circulation" change is defined as being the sum of the intraclass changes of each type weighted by the corresponding 1960-1999 mean frequency of the GCM. The "total" change takes both the intraclass changes and the frequency changes into account. In the case of SLP, the circulation changes counteract the SLP decrease over the NW quarter by approximately 50 % (Table 3). This means that, without the projected frequency/circulation changes, the SLP decrease would be twice as strong as it is projected to be. Over the SE quarter, the changes in frequency slightly strengthen the SLP decrease by favouring Type 1 (negative SLP anomaly) to the detriment of Type 2 (positive SLP anomaly). Over the two other quarters, the circulation changes have no significant impact on the SLP decrease.

The analysis of the intraclass changes for each GCM separately shows that the GCMs are more in agreement over the southern part of the domain, than over the northern part (see Figs. F and J in the Supplementary Material for RCP4.5 and RCP8.5 respectively). For the NW quarter, the SLP changes are very different from one GCM to another. While 13 GCMs project a decrease in SLP for Type 1, there are only 9 GCMs simulating an SLP decrease for Types 2 and 3. The total SLP change resulting from changes in intraclass SLP and circulation

type frequencies is projected to be positive by 8 GCMs. This represents only the half of the GCM panel used here, so that the confidence in this change is low. For the north-eastern part of the domain, 11 GCMs project a decrease in SLP for Type 1, and 10 GCMs project a decrease in SLP for Types 2, 3, and the resulting seasonal mean. The projections are more uniform over the SW and SE quarters, where 12 GCMs simulate an SLP decrease for all types.

4.2.3 Temperature

The TAS anomaly intraclass changes show a strong increase, which is similar for all parts of the domain and all circulation types, despite that Type 1, which induces lower temperatures than normal, is projected to have a slightly more pronounced warming than Type 2 (see Fig. 8 ; see also Fig. C in the Supplementary Material for RCP4.5). Thus, the warming is projected to affect all circulation situations in a similar manner. When analysing the impact of the circulation type frequency changes on the change in TAS anomaly, it appears that the projected increase in the frequency of Type 1 (inducing colder conditions than normal) to the detriment of Type 2 (warmer conditions) should not significantly affect the TAS increase (see Table 3). This can be explained by the low differentiation between the intraclass means of Types 1 and 2, and the slightly more pronounced warming for Type 1 compared to Type 2. As suspected, the separated analysis of the GCM projections shows that all GCMs project a warming for all types over all regions (see Figs. G and K in the Supplementary Material for RCP4.5 and RCP8.5 respectively). However, as for SLP, Fig. 4 shows great differences among GCMs in the magnitude of the warming, ranging from +2°C to more than +6°C for RCP8.5.

4.2.4 Precipitation

The changes in PR anomaly show important differences among the subdomains (see Fig. 2 ; see also Fig. D in the Supplementary Material for RCP4.5). All the types project a PR increase in the NW quarter and a drying of the Mediterranean region and the continental (eastern) part of the domain in summer. As for SLP, the circulation changes significantly influence the PR projections for the NW quarter. In fact, the frequency increase of Type 1 (inducing drier conditions) to the detriment of Type 2 (inducing wetter conditions) counters the PR increase, despite the intraclass PR increase for all types, resulting in a mitigated PR decrease (see Table 3). For the other subdomains, the changes in PR anomaly show a PR decrease and the circulation changes are not projected to significantly affect the PR changes. These results confirm the simulations made by Rowell and Jones (2006) based on only one regional climate model using the A2 SRES (Special Report on Emissions Scenarios) scenario. They showed that, over the British Isles, the PR increase due to the warming (here the intraclass changes) is opposed to the PR decrease due to circulation changes. They conclude that, over the Mediterranean region and eastern Europe, drying is projected to be attributable to other processes like soil moisture decrease and the warming itself, rather than to circulation changes.

Furthermore, as Rowell and Jones (2006), we have low confidence in the circulation change, and consequently also in its impact on PR, since the projected circulation changes are not unanimous among the GCMs, as said above. It even remains unclear whether PR will increase or decrease over the NW quarter. The analysis of each GCM separately shows that, while the 14-GCM ensemble shows a PR increase with increasing TAS for all types, 9 GCMs project a PR decrease for Types 1 and 3, and only 8 GCMs project a PR increase for Type 2 (see Figs. H and L in the Supplementary Material for RCP4.5 and RCP8.5 respectively). The resulting

total PR change over the NW quarter is projected to be negative by 10 GCMs. Nevertheless, with regard to all uncertainties pointed out, it remains unclear whether the intraclass PR increase resulting from rising temperatures (inducing higher evaporation, higher atmospheric water content and then higher PR) or the PR decrease due to the circulation changes will be dominant in the NW subdomain. Over the NE quarter, the uncertainties among the GCMs are also very high. Only one GCM out of two projects a PR decrease for Type 1, while there are still 4 GCMs projecting a PR increase for types 2 and 3, and for the seasonal mean. The drying of the Mediterranean region (i.e. SW and SE quarter) is much more consistent. The only GCM projecting a not significant PR increase for Types 2 and 3, and the seasonal mean over the SE quarter is CNRM-CM5, one of the least successful GCMs in our ranking. Over the western Mediterranean and the Iberian peninsula (SW quarter), all GCMs project a PR decrease, except MIROC-ESM, which projects a non significant PR increase for Type 1. Again, Fig. 3 shows great differences among GCMs, which project opposite PR changes for the future. Furthermore, the magnitude of the projected PR changes over 2060-2099 is lower than the GCM biases over the historical period, which adds even more doubt about the reliability of the projected PR changes.

5. Discussion and conclusion

In this study, we have used an automatic circulation type classification based on the Spearman rank correlation to evaluate at a daily timescale the atmospheric circulation at sea level simulated by 14 CMIP5 GCMs over Europe for the historical reference period (1960-1999) in summer (June, July, and August). This approach was also used to analyse the future projections of the atmospheric circulation at sea level and the related changes in near-surface temperature, precipitation and sea level pressure.

For the historical reference period, we showed that the differences in circulation type frequency between the ERA-40 based SLP, used as the reference dataset, and the GCMs are generally very large. Furthermore, we cannot identify a particular GCM as performing the overall best, as also stated by Casado and Pastor (2012) and Stoner *et al.* (2009). In general, the GCMs seem to have difficulty in reproducing the observed frequencies of the circulation types over Europe in summer.

For the future projections, significant changes towards a slight weakening of the depression over the British Isles/North Sea and a diminution of SLP over the Mediterranean region have been detected. In addition to the frequency changes of some circulation types, intraclass changes of all variables used here (SLP, TAS, and PR) are observed. For SLP, a decrease is projected over the whole domain as a result of higher TAS. The PR intraclass changes indicate a drying over eastern Europe and the Mediterranean region, and an increase in PR over the NW part of the domain. The TAS projections show a strong increase towards the end of this century. In general, these intraclass changes are of the same order as the resulting average changes. Thus, the circulation changes do not significantly affect the projections of TAS. Nevertheless, two exceptions have been pointed out. For SLP, the circulation changes mitigate the decrease over north-western Europe by favouring the circulation type that has a positive SLP anomaly over this region. For PR, the increase projected on basis of the intraclass changes over the NW quarter is countered by a higher frequency of the "dryer" Type 1 to the detriment of the "wetter" Type 2. However, there are high uncertainties among the GCM circulation, SLP, and PR changes. Thus, our confidence in the SLP and PR changes and, in particular, in the mitigating or enhancing role of the circulation changes on these variables over the NW quarter, is very low as all the GCMs do not agree. This is confirmed by Hawkins

and Sutton (2011), who showed that the uncertainty associated with PR projections under climate change conditions is generally higher than the magnitude of the change itself.

The projected changes detected for the CMIP5 GCMs used here, and in particular the SLP and PR changes, show the same trends as highlighted in the IPCC AR4 (Meehl *et al.*, 2007, and Christensen *et al.*, 2007) using CMIP3 GCMs. The higher spatial resolution, new future experiments, and other improvements in the physical basis of the CMIP5 GCMs compared to the previous CMIP3 GCM generation, seem not to have a significant influence on the evolution of the variables used here under global warming conditions.

Our results suggest that the general circulation changes are projected to affect changes in PR, but the impact of these changes is only marked over the NW quarter, where the circulation types are the most differentiated. This suggests that the atmospheric circulation is an important driver of the meteorological conditions over north-western Europe, but this influence decreases towards the south-east of the domain, where the changes are only driven by the temperature increase. The decrease of SLP influence on ground variables towards the south-east of Europe is explained by the low variability in SLP over this region, compared to the NW quarter of the domain.

Finally, the range of the SLP and PR anomalies with regard to the TAS anomalies over the GCMs is relatively high. This shows that the relationship between the variables differs from one GCM to another, even within a same scenario (e.g. RCP8.5). Thus, it is important to use several GCMs, in order to have an idea of the uncertainty due to internal physics and parameterization of the GCMs. Furthermore, we showed that, due to the spread of the GCM projections, it is very dangerous to use a simple multi-model ensemble, without an analysis of

the GCMs being part of this ensemble. This joins the findings of Hawkins and Sutton (2009) and Hawkins and Sutton (2011), who showed for TAS (resp. PR) that the uncertainty due to the spread of the values between GCMs dominates the uncertainty due to the scenarios.

Acknowledgements

We acknowledge the World Climate Research Programme's Working Group on Coupled Modelling, which is responsible for CMIP, and we thank the climate modelling groups for producing and making available their model output. For CMIP the U.S. Department of Energy's Program for Climate Model Diagnosis and Intercomparison provides coordinating support and led development of software infrastructure in partnership with the Global Organization for Earth System Science Portals. The ECMWF ERA-40 Reanalysis data used in this study were obtained from the ECMWF Data Server (http://www.ecmwf.int). NCEP/NCAR Reanalysis data were provided by the NOAA/OAR/ESRL PSD, Boulder, Colorado, USA, from their website at http://www.esrl.noaa.gov/psd/.

Bibliography

Anagnostopoulou C, Tolika K, Maheras P, Kutiel H, Flocas H. 2008. Performance of the general circulation HadAM3P model in simulating circulation types over the Mediterranean region. *International Journal of Climatology* **28:** 185-203. DOI: 10.1002/joc.1521.

Anagnostopoulou C, Tolika K, Maheras P. 2009. Classification of circulation types: a new flexible automated approach applicable to NCEP and GCM datasets. *Theoretical and Applied Climatology* **96:** 3-15. DOI: 10.1007/s00704-008-0032-6.

Bardossy A, Caspary H-J. 1990. Detection of climate change in Europe by analyzing European atmospheric circulation patterns from 1881 to 1989. *Theoretical and Applied Climatology* **42:** 155-167.

Bardossy A, Stehlik J, Caspary H-J. 2002. Automated objective classification of daily circulation patterns for precipitation and temperature downscaling based on optimized fuzzy rules. *Climate Research* **23:** 11-22. DOI: 10.3354/cr023011.

Belleflamme A, Fettweis X, Lang C, Erpicum M. 2013. Current and future atmospheric circulation at 500 hPa over Greenland simulated by the CMIP3 and CMIP5 global models. *Climate Dynamics* **41:** 2061-2080. DOI: 10.1007/s00382-012-1538-2.

Casado M, Pastor M. 2012. Use of variability modes to evaluate AR4 climate models over the Euro-Atlantic region. *Climate Dynamics* **38:** 225-237. DOI: 10.1007/s00382-011-1077-2.

Christensen J, Hewitson B, Busuioc A, Chen A, Gao X, Held I, Jones R, Kolli R, Kwon W-T, Laprise R, Magaña Rueda V, Mearns L, Menéndez C, Räisänen J, Rinke A, Sarr A, Whetton P. 2007. *Regional Climate Projections*. In: *Climate Change 2007: The Physical Science Basis. Contribution of Working Group I to the Fourth Assessment Report of the Intergovernmental Panel on Climate Change.* [Solomon S, Qin D, Manning M, Chen Z, Marquis M, Averyt K, Tignor M, Miller H (eds.)] (Cambridge University Press: Cambridge) United Kingdom and New York, NY, USA.

Demuzere M, Werner M, van Lipzig N, Roeckner E. 2009. An analysis of present and future ECHAM5 pressure fields using a classification of circulation patterns. *International Journal*

of Climatology **29:** 1796-1810. DOI: 10.1002/joc.1821.

Fettweis X, Mabille G, Erpicum M, Nicolay S, Van den Broeke M. 2011. The 1958-2009 Greenland ice sheet surface melt and the mid-tropospheric atmospheric circulation. *Climate Dynamics* **36:** 139-159. DOI: 10.1007/s00382-010-0772-8.

Fettweis X, Hanna E, Lang C, Belleflamme A, Erpicum M, Gallée H. 2013. Important role of the mid-tropospheric atmospheric circulation in the recent surface melt increase over the Greenland ice sheet. *The Cryosphere* **7:** 241-248. DOI: 10.5194/tc-7-241-2013.

Hawkins E, Sutton R. 2009. The potential to narrow uncertainty in regional climate predictions. *Bulletin of the American Meteorological Society* **90:** 1095-1107. DOI: 10.1175/2009BAMS2607.1.

Hawkins E, Sutton R. 2011. The potential to narrow uncertainty in projections of regional precipitation change. *Climate Dynamics* **37:** 407-418. DOI: 10.1007/s00382-010-0810-6.

Huth R. 2000. A circulation classification scheme applicable in GCM studies. *Theoretical and Applied Climatology* **67:** 1-18. DOI: 10.1007/s007040070012.

Huth R, Beck C, Philipp A, Demuzere M, Ustrnul Z, Cahynová M, Kyselý J, Tveito OE. 2008. Classifications of atmospheric circulation patterns: Recent advances and applications. *Annals of the New York Academy of Sciences* **1146:** 105-152. DOI: 10.1196/annals.1446.019.

Kalnay E, Kanamitsu M, Kistler R, Collins W, Deaven D, Gandin L, Iredell M, Saha S, White

G, Woollen J, Zhu Y, Leetmaa A, Reynolds B, Chelliah M, Ebisuzaki W, Higgins W, Janowiak J, Mo K, Ropelewski C, Wang J, Jenne R, Joseph D. 1996. The NCEP/NCAR 40-Year Reanalysis Project. *Bulletin of the American Meteorological Society* **77:** 437-471. DOI: 10.1175/1520-0477(1996)077<0437:TNYRP>2.0.CO;2.

Kyselý J, Huth R. 2006. Changes in atmospheric circulation over Europe detected by objective and subjective methods. *Theoretical and Applied Climatology* **85:** 19-36. DOI: 10.1007/s00704-005-0164-x.

Meehl G, Tebaldi C. 2004. More intense, more frequent, and longer lasting heat waves in the 21st century. *Science* **305:** 994-997. DOI: 10.1126/science.1098704.

Meehl G, Stocker T, Collins W, Friedlingstein P, Gaye A, Gregory J, Kitoh A, Knutti R, Murphy J, Noda A, Raper S, Watterson I, Weaver A, Zhao Z-C. 2007. *Global Climate Projections.* In: *Climate Change 2007: The Physical Science Basis. Contribution of Working Group I to the Fourth Assessment Report of the Intergovernmental Panel on Climate Change.* [Solomon S, Qin D, Manning M, Chen Z, Marquis M, Averyt K, Tignor M, Miller H (eds.)] (Cambridge University Press: Cambridge) United Kingdom and New York, NY, USA.

Moss R, Edmonds J, Hibbard K, Manning M, Rose S, van Vuuren D, Carter T, Emori S, Kainuma M, Kram T, Meehl G, Mitchell J, Nakicenovic N, Riahi K, Smith S, Stouffer R, Thomson A, Weyant J, Wilbanks T. 2010. The next generation of scenarios for climate change research and assessment. *Nature* **463:** 747-756. DOI: 10.1038/nature08823.

Pasini A, Langone R. 2012. Influence of circulation patterns on temperature behavior at the

regional scale: A case study investigated via neural network modeling. *Journal of Climate* **25:** 2123-2128. DOI: 10.1175/JCLI-D-11-00551.1.

Pastor M, Casado M. 2012. Use of circulation types classifications to evaluate AR4 climate models over the Euro-Atlantic region. *Climate Dynamics*. DOI: 10.1007/s00382-012-1449-2.

Philipp A, Della-Marta P, Jacobeit J, Fereday D, Jones P, Moberg A, Wanner H. 2007. Long-term variability of daily North Atlantic-European pressure patterns since 1850 classified by simulated annealing clustering. *Journal of Climate* **20:** 4065-4095. DOI: 10.1175/JCLI4175.1.

Philipp A, Bartholy J, Beck C, Erpicum M, Esteban P, Fettweis X, Huth R, James P, Jourdain S, Kreienkamp F, Krennert T, Lykoudis S, Michalides S, Pianko K, Post P, Rassilla Àlvarez D, Schiemann R, Spekat A, Tymvios FS. 2010. COST733CAT - a database of weather and circulation type classifications. *Physics and Chemistry of the Earth* **35:** 360-373. DOI: 10.1016/j.pce.2009.12.010.

Rowell D, Jones R. 2006. Causes and uncertainty of future summer drying over Europe. *Climate Dynamics* **27:** 281-299. DOI: 10.1007/s00382-006-0125-9.

Stoner AM, Hayhoe K, Wuebbles D. 2009. Assessing General Circulation Model simulations of atmospheric teleconnection patterns. *Journal of Climate* **22:** 4348-4372. DOI: 10.1175/2009JCLI2577.1.

Uppala SM, Kallberg PW, Simmons AJ, Andrae U, da Costa Bechtold V, Fiorino M, Gibson JK, Haseler J, Hernandez A, Kelly GA, Li X, Onogi K, Saarinen S, Sokka N, Allan RP,

Andersson E, Arpe K, Balmaseda MA, Beljaars ACM, van de Berg L, Bidlot J, Bormann N, Caires S, Chevallier F, Dethof A, Dragosavac M, Fisher M, Fuentes M, Hagemann S, Holm E, Hoskins B, Isaksen L, Janssen PAEM, Jenne R, McNally AP, Mahfouf J-F, Morcrette J-J, Rayner NA, Saunders RW, Simon P, Sterl A, Trenberth KE, Untch A, Vasiljevic D, Viterbo P, Woollen J. 2005. The ECMWF re-analysis. *Quarterly Journal of the Royal Meteorological Society* **131:** 2961-3012. DOI: 10.1256/qj.04.176.

Tables

Table 1: All data have been retrieved from the CMIP5 data base website http://pcmdi3.llnl.gov/esgcet.

GCM name	Spatial resolution (lat x lon)	Research centre ID (Country)
BCC-CSM1-1	2.8° x 2.8°	BCC (China)
BNU-ESM	2.8° x 2.8°	BNU (China)
CanESM2	2.8° x 2.8°	CCCma (Canada)
CNRM-CM5	1.4° x 1.4°	CNRM-CERFACS (France)
GFDL-ESM2M	2.0° x 2.5°	NOAA GFDL (United States)
HadGEM2-CC	1.25° x 1.875°	MOHC (United Kingdom)
IPSL-CM5A-LR	1.875° x 3.75°	IPSL (France)
IPSL-CM5A-MR	1.25° x 2.5°	IPSL (France)
MIROC-ESM-CHEM	2.8° x 2.8°	MIROC (Japan)
MIROC-ESM	2.8° x 2.8°	MIROC (Japan)
MPI-ESM-LR	1.875° x 1.875°	MPI-M (Germany)
MPI-ESM-MR	1.875° x 1.875°	MPI-M (Germany)
MRI-CGCM3	1.125° x 1.125°	MRI (Japan)
NorESM1-M	1.875° x 2.5°	NCC (Norway)

Table 2: The frequency (in %) of the circulation types is calculated over the 1960-1999 period. The root mean square error (RMSE) is computed on the frequency differences between the GCM types and the ERA-40 (resp. NCEP/NCAR) reference types. The ranking of the GCMs is determined on basis of this RMSE. The NCEP/NCAR (resp. ERA-40) RMSE based on the ERA-40 (resp. NCEP/NCAR) classification is shown for comparison.

	ERA-40					NCEP/NCAR				
Model name	Type 1	Type 2	Type 3	RMSE	Ranking	Type 1	Type 2	Type 3	RMSE	Ranking
ERA-40	25.7	36.2	38.1			34.0	30.1	35.9	0.69	
NCEP/NCAR	25.4	34.7	40.0	1.41		34.8	29.1	36.1		
BCC-CSM1-1	25.1	32.9	42.0	2.96	1	36.2	27.7	36.1	1.16	1
BNU-ESM	27.8	38.3	33.9	2.98	2	40.9	30.0	29.1	5.40	7
CanESM2	35.1	22.8	42.1	9.75	10	45.7	17.4	36.9	9.27	10
CNRM-CM5	21.9	23.8	54.4	12.03	12	29.6	20.7	49.7	9.68	11
GFDL-ESM2M	17.6	34.7	47.8	7.37	7	28.2	31.3	40.5	4.71	5
HadGEM2-CC	28.0	28.5	43.6	5.65	6	38.5	21.9	39.7	5.13	6
IPSL-CM5A-LR	18.7	21.0	60.3	16.07	14	23.2	19.9	56.9	14.71	14
IPSL-CM5A-MR	28.0	25.2	46.8	8.21	9	34.0	22.5	43.5	5.76	8
MIROC-ESM-CHEM	26.1	30.4	43.5	4.57	4	39.2	25.9	34.9	3.23	2
MIROC-ESM	25.4	32.3	42.3	3.34	3	40.1	25.1	34.8	3.93	3
MPI-ESM-LR	16.9	52.7	30.4	11.64	11	31.1	44.6	24.3	11.43	12
MPI-ESM-MR	14.5	56.7	28.8	14.47	13	28.3	48.3	23.4	13.80	13
MRI-CGCM3	18.4	32.8	48.8	7.72	8	25.3	29.6	45.1	7.57	9
NorESM1-M	19.2	41.6	39.2	4.91	5	31.6	35.2	33.2	4.26	4

Table 3: The “total” and the “no circulation” changes are calculated over the RCP8.5 yearly means for which the total TAS increase exceeds 4 K with regard to the 1960-1999 JJA mean. The “total” change corresponds to the black (T) dots on Figs. 2, 7, and 8. The “no circulation” change corresponds to the weighted sum of the blue (1), green (2), and red (3) dots on Figs. 2, 7, and 8. The pairs of values in bold are significantly different from each other following a Student t-test at a 5 % confidence level.

	NW		NE		SW		SE	
	Total	No circ.	Total	No circ.	Total	No circ.	Total	No circ.
SLP (hPa)	**-0.62**	**-1.47**	-1.34	-1.35	-1.81	-1.88	**-2.18**	**-1.94**
TAS (K)	5.11	5.04	5.79	5.80	5.64	5.57	5.77	5.76
PR (mm/day)	**-0.05**	**0.14**	-0.16	-0.20	-0.31	-0.30	-0.26	-0.30

Figures

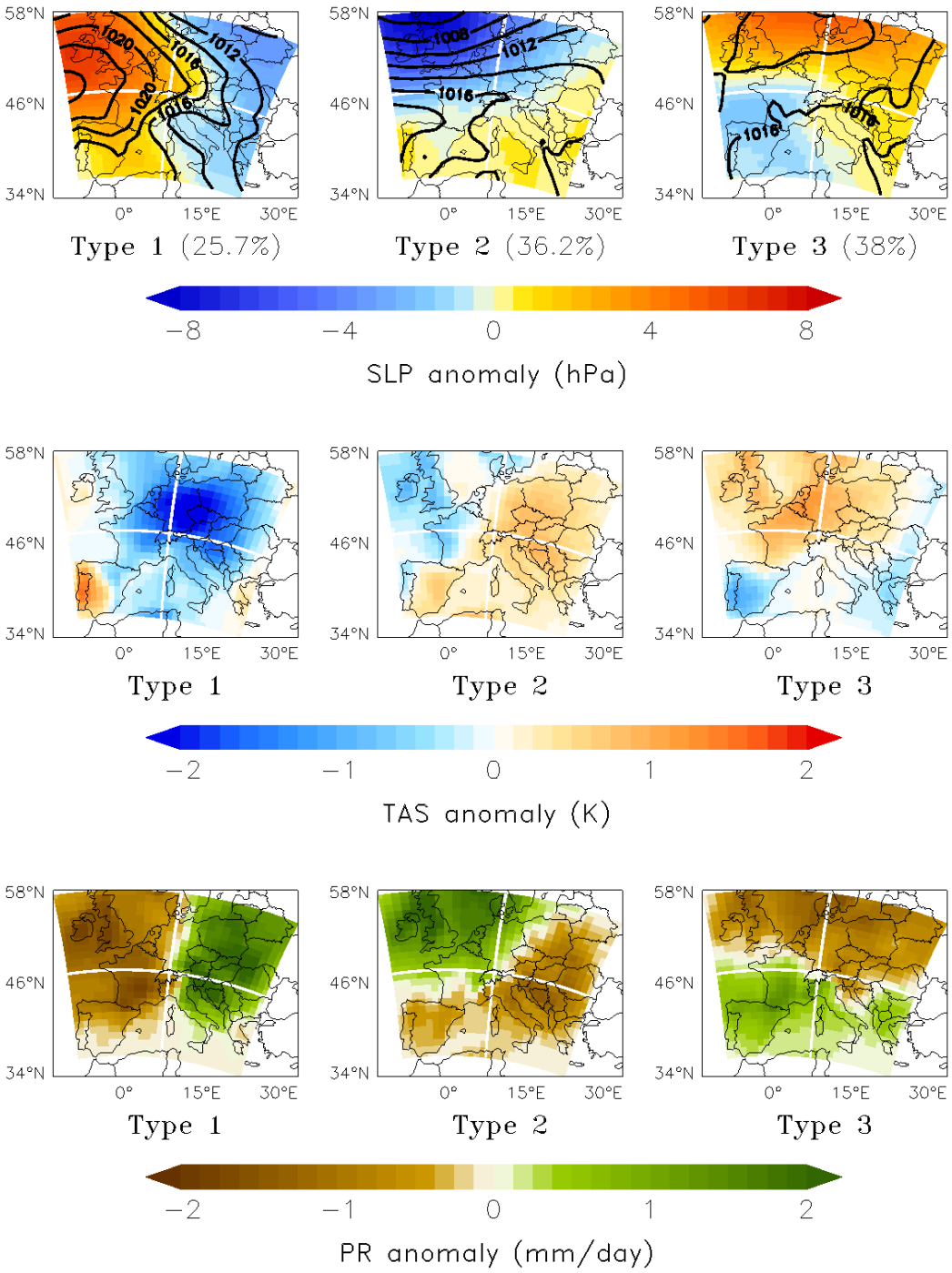

Figure 1: Top: the JJA circulation types over 1960-1999 from the SLP based automatic circulation type classification using ERA-40 over Europe are represented by the solid black isobars (in hPa). The relative frequency (in percent) of each type is shown in brackets. The background colours show the anomaly of each type with regard to the JJA mean over 1960-1999, for SLP (top), TAS (middle), and PR (bottom).

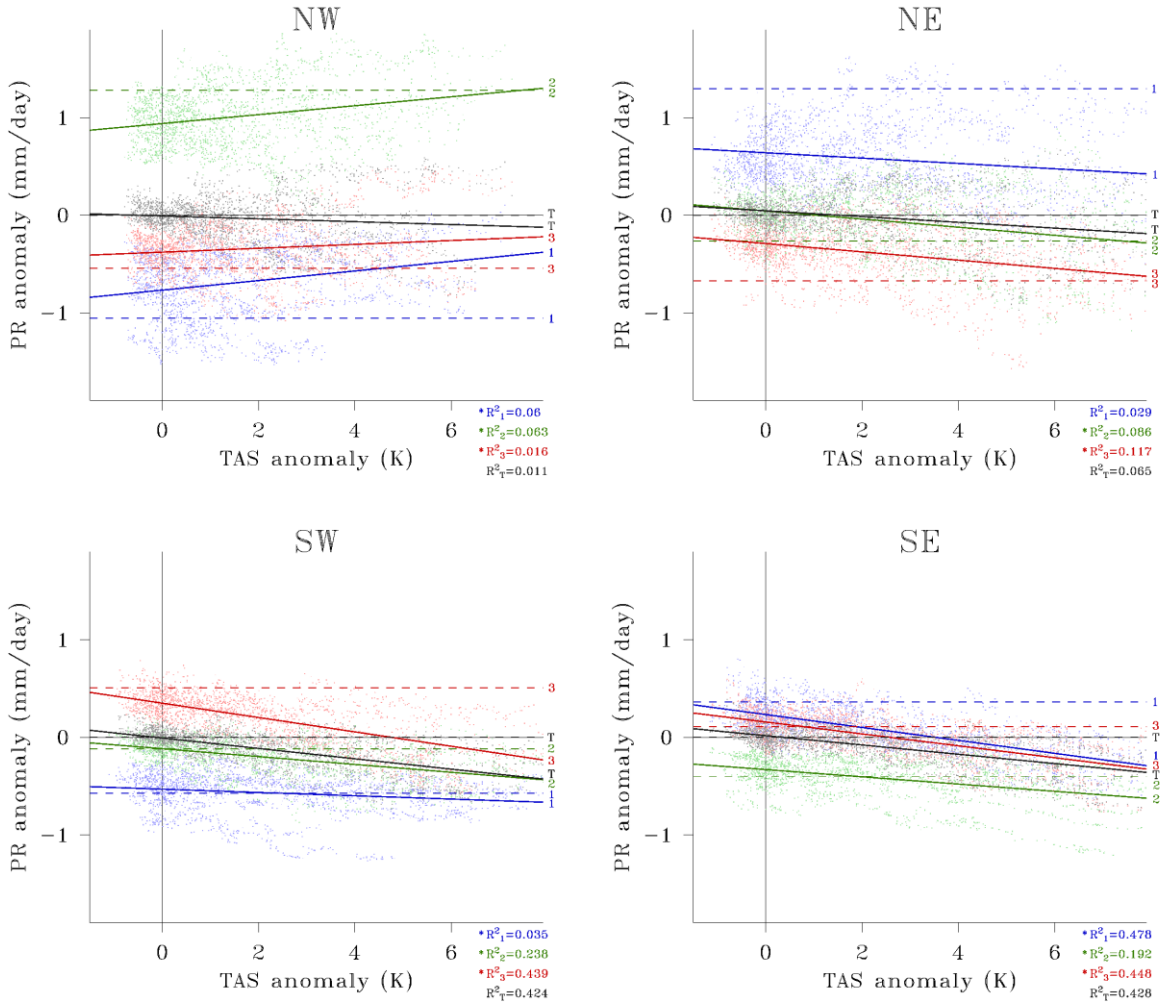

Figure 2: The dots represent the yearly GCM PR anomaly (with regard to the JJA 1960-1999 mean and after a 10-year running mean) as a function of the total (i.e. over all Types) TAS change with regard to the JJA 1960-1999 mean using the Historical experiment (1951-2005) and the future projection RCP8.5 experiment (2006-2100). A linear regression line for the CMIP5 ensemble mean is plotted for each type (1, 2, and 3) and the total yearly mean (T) (see the determination coefficients). (*) indicates that the regression slope of a given type is significantly different from the (black) total slope following a Student t-test at a 5 % confidence level. The ERA-40 reference PR anomalies (JJA, 1960-1999) are represented by the dashed lines.

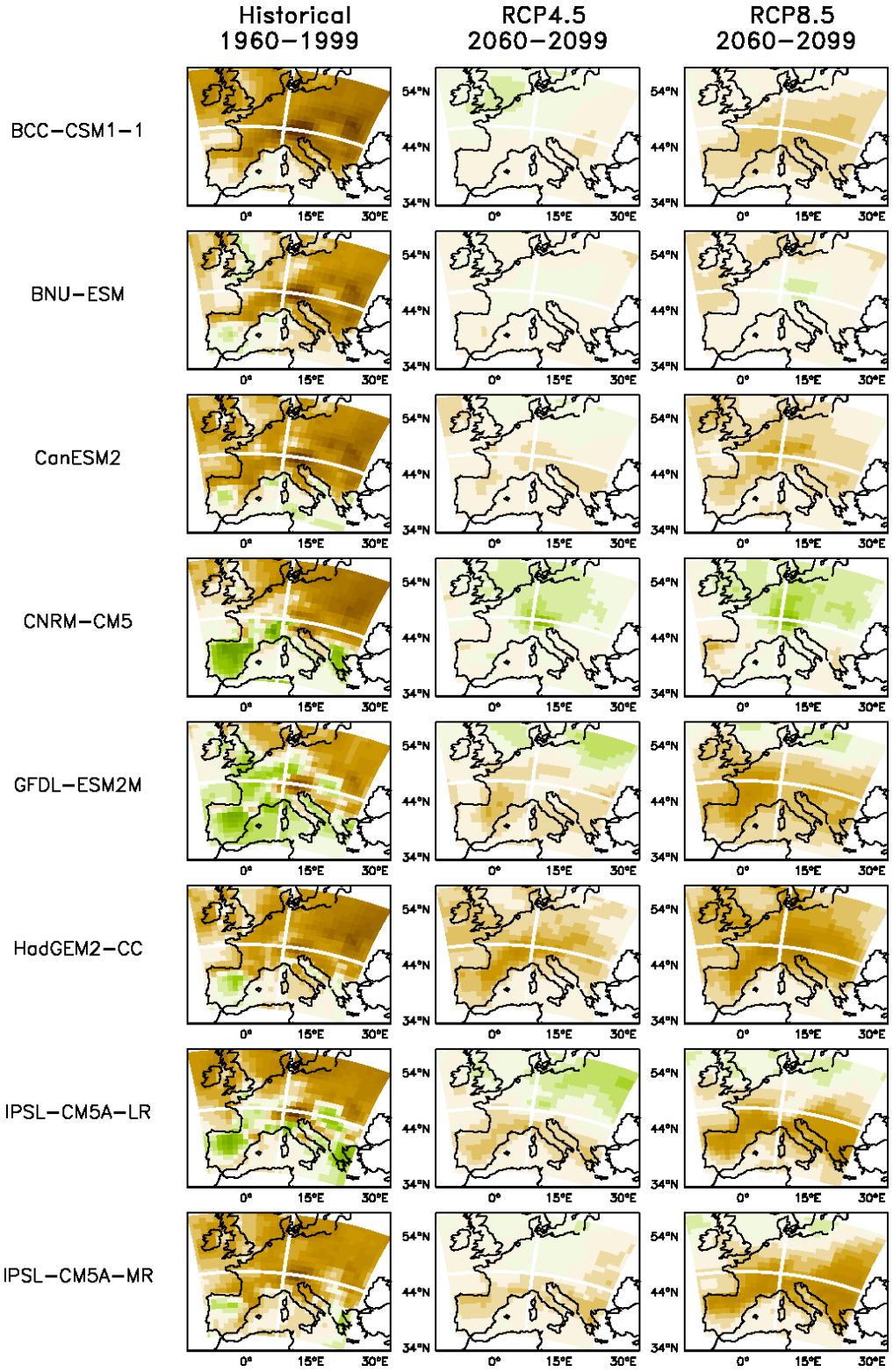

Figure 3: For each GCM and the 14-GCM ensemble mean, the PR bias over the historical reference period (1960-1999, JJA) is calculated with regard to ERA-40. The RCP4.5 (resp. RCP8.5) PR change over 2060-2099 (JJA) is computed with regard to the historical reference mean (1960-1999, JJA) of the GCM.

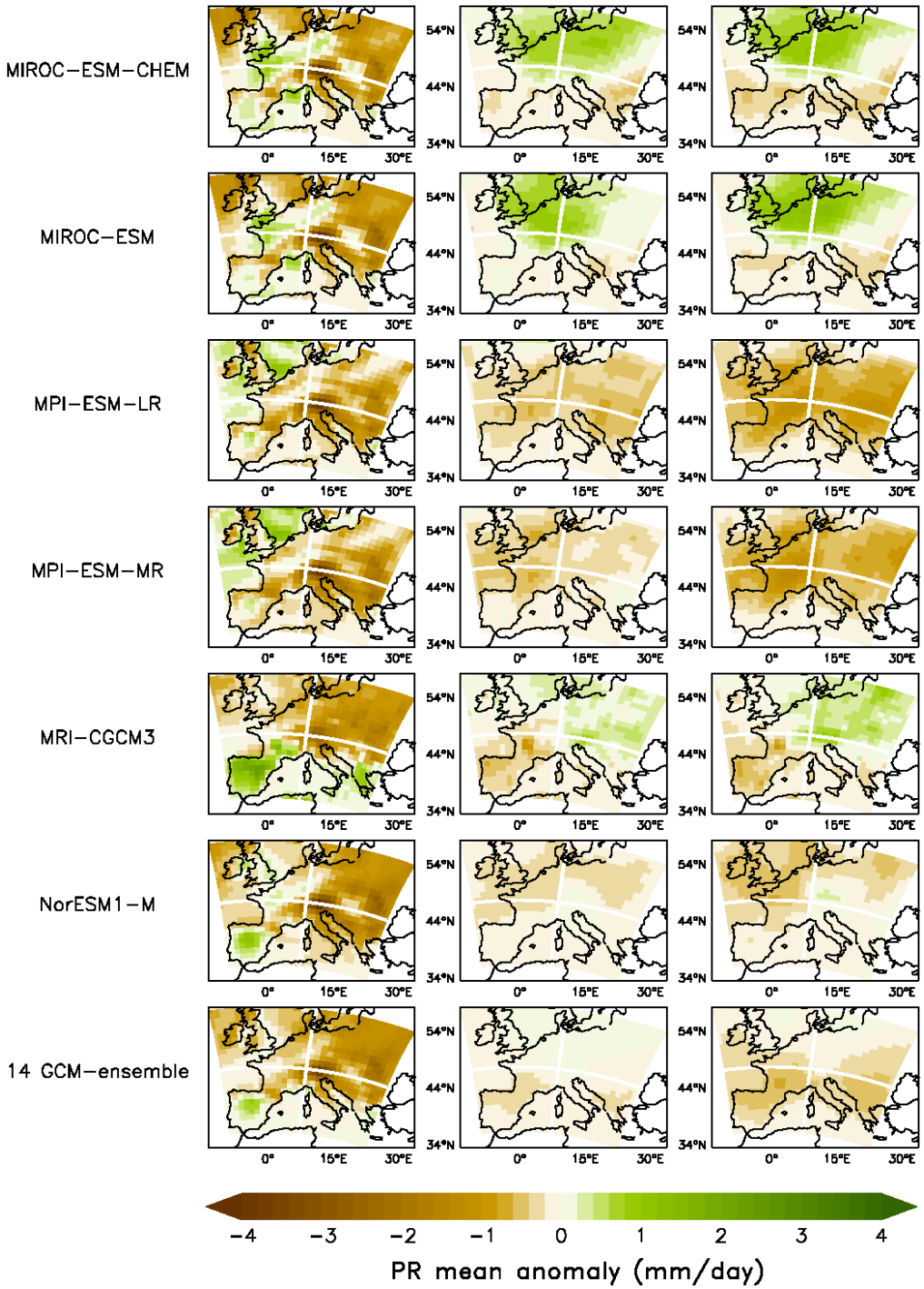

Figure 3: continued.

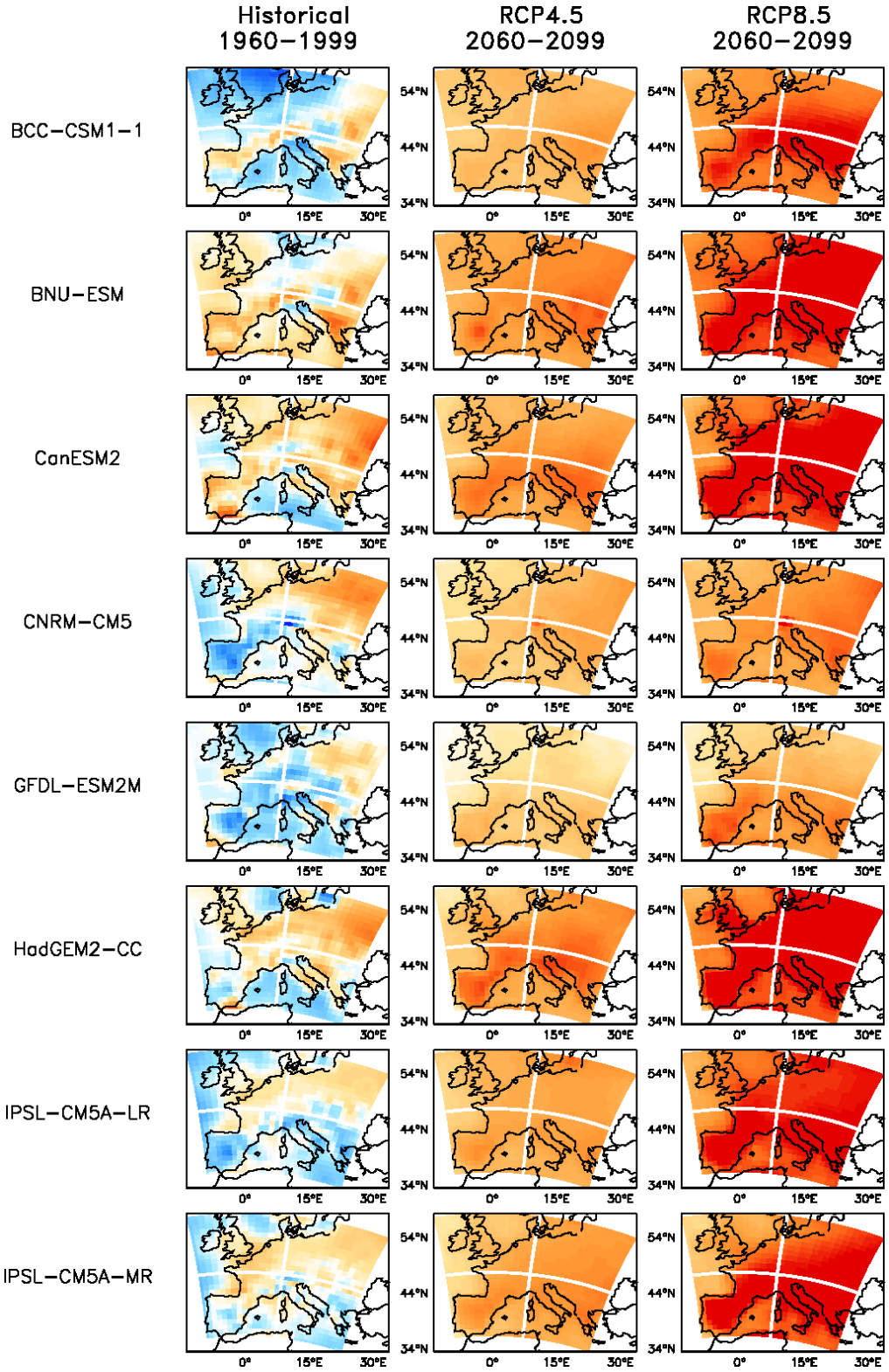

Figure 4: For each GCM and the 14-GCM ensemble mean, the TAS bias over the historical reference period (1960-1999, JJA) is calculated with regard to ERA-40. The RCP4.5 (resp. RCP8.5) TAS change over 2060-2099 (JJA) is computed with regard to the historical reference mean (1960-1999, JJA) of the GCM.

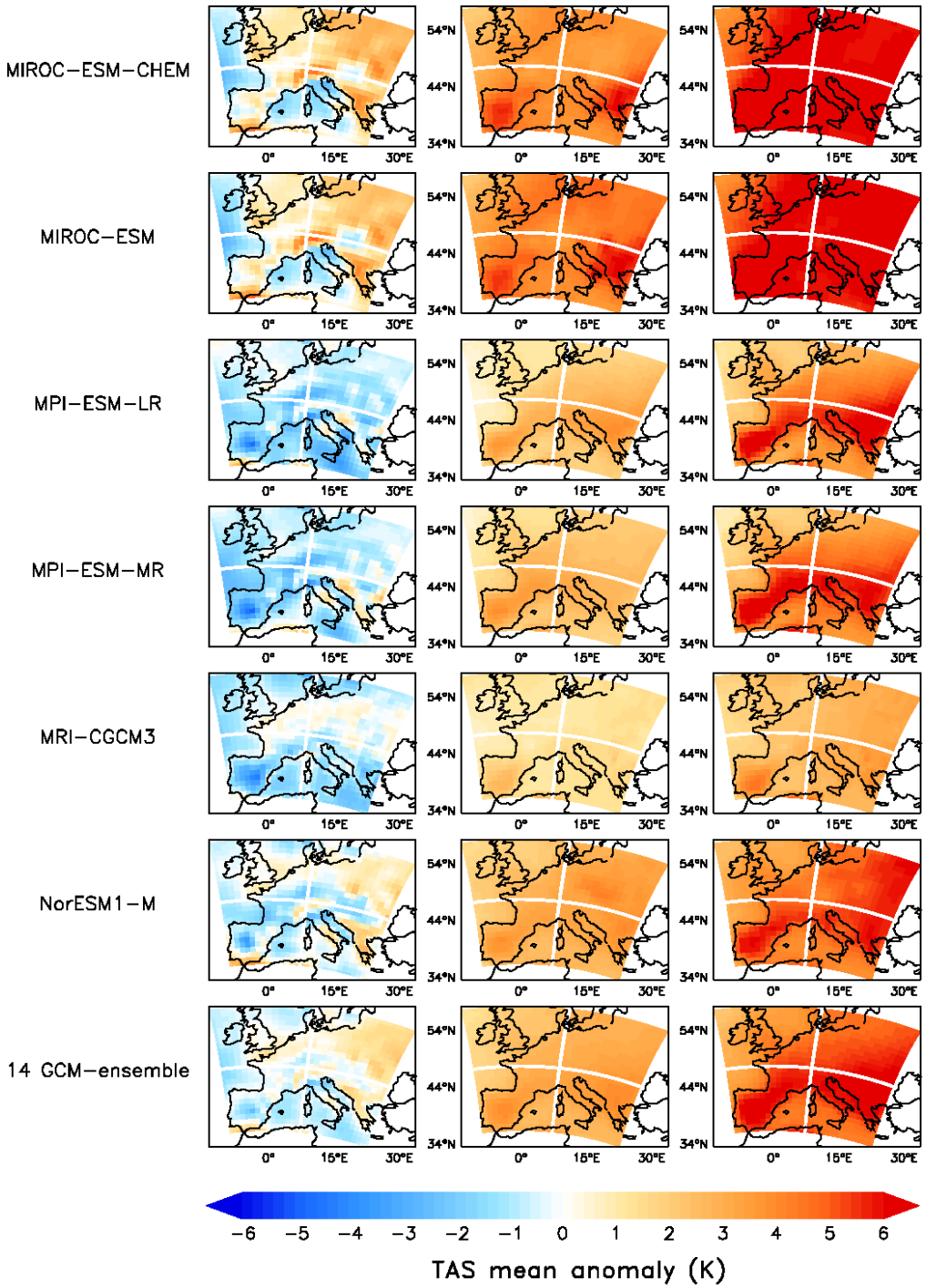

Figure 4: continued.

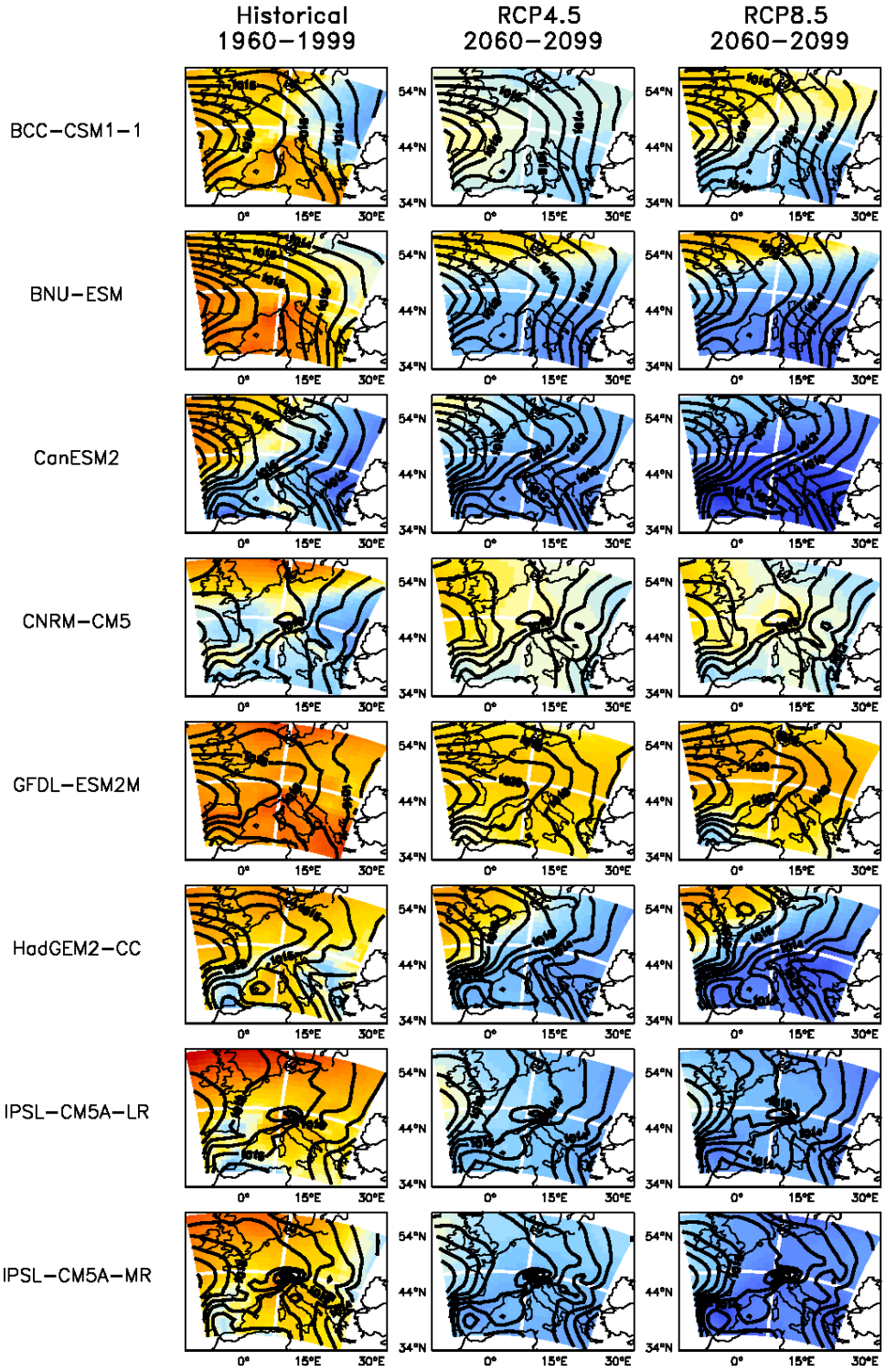

Figure 5: For each GCM and the 14-GCM ensemble mean, the SLP bias over the historical reference period (1960-1999, JJA) is calculated with regard to ERA-40 (shades). The RCP4.5 (resp. RCP8.5) SLP change over 2060-2099 (JJA) is computed with regard to the historical reference mean (1960-1999, JJA) of the GCM (shades). The black isobars show the mean SLP over 1960-1999, JJA (resp. 2060-2099, JJA) (in hPa).

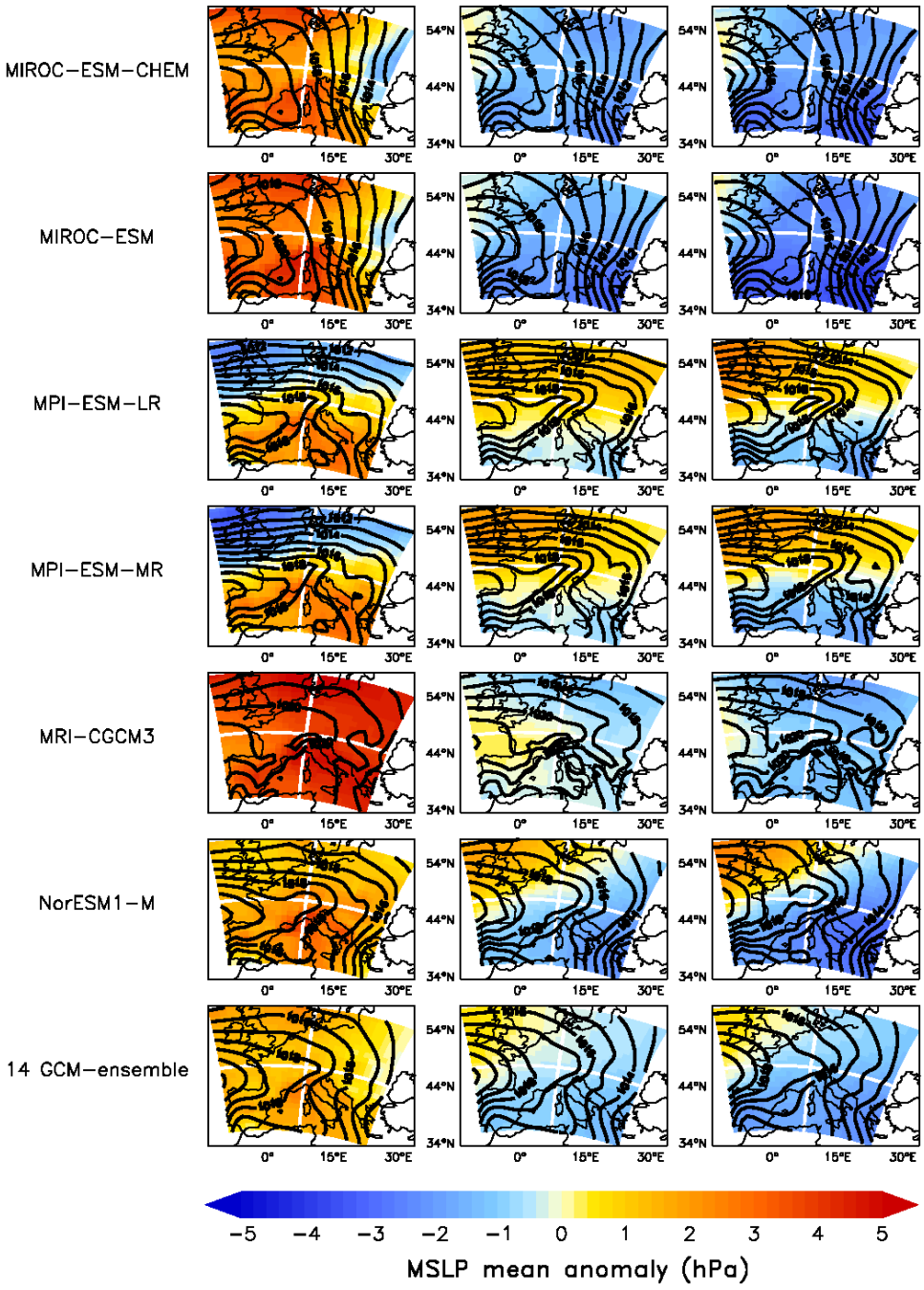

Figure 5: continued.

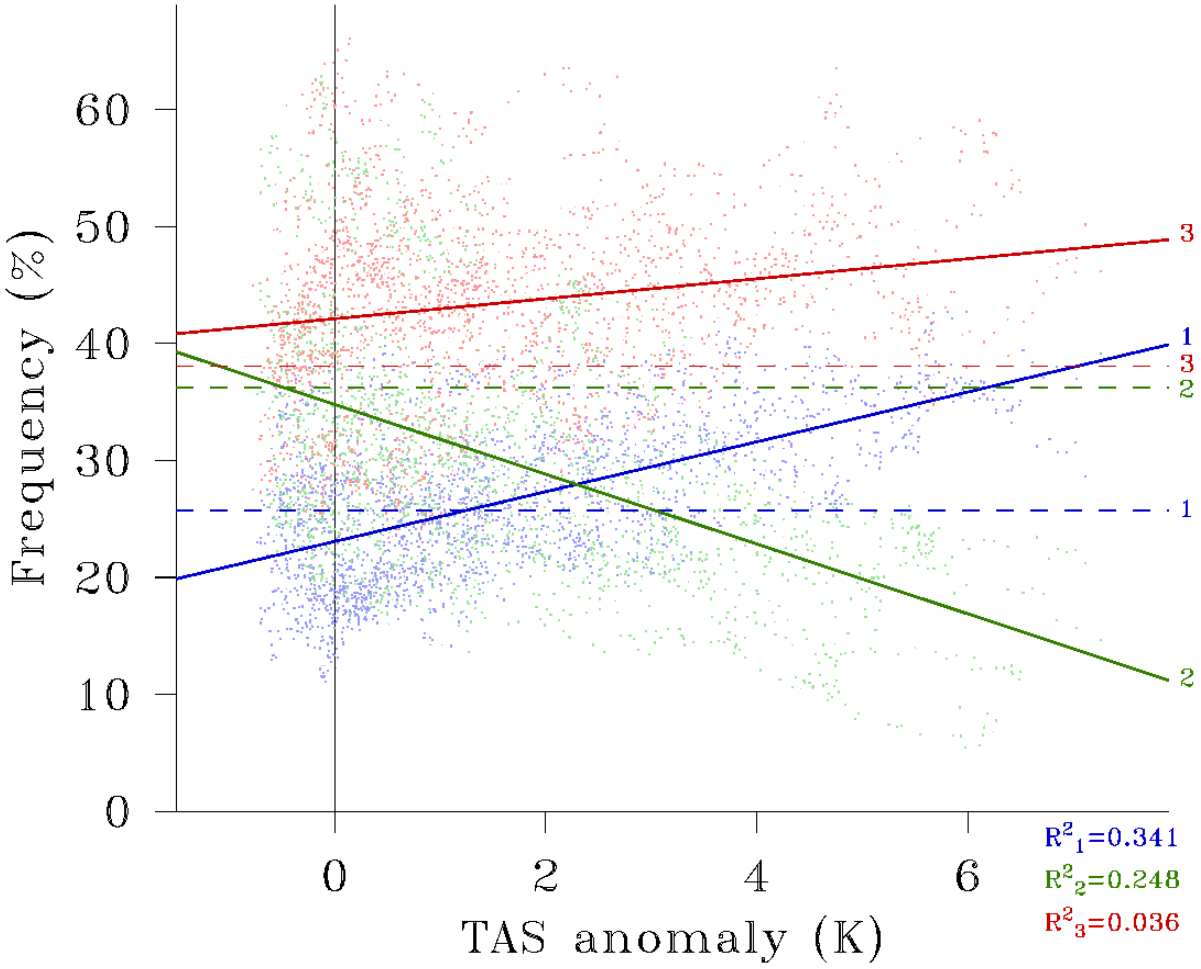

Figure 6: The dots represent the yearly GCM frequencies (after a 10-year running mean) as a function of the total (i.e. over all Types) TAS change with regard to the JJA 1960-1999 mean using the Historical experiment (1951-2005) and the future projection RCP8.5 experiment (2006-2100). A linear regression line for the CMIP5 ensemble mean is plotted for each type (1, 2, and 3) (see the determination coefficients). The ERA-40 reference frequencies (JJA, 1960-1999) are represented by the dashed lines.

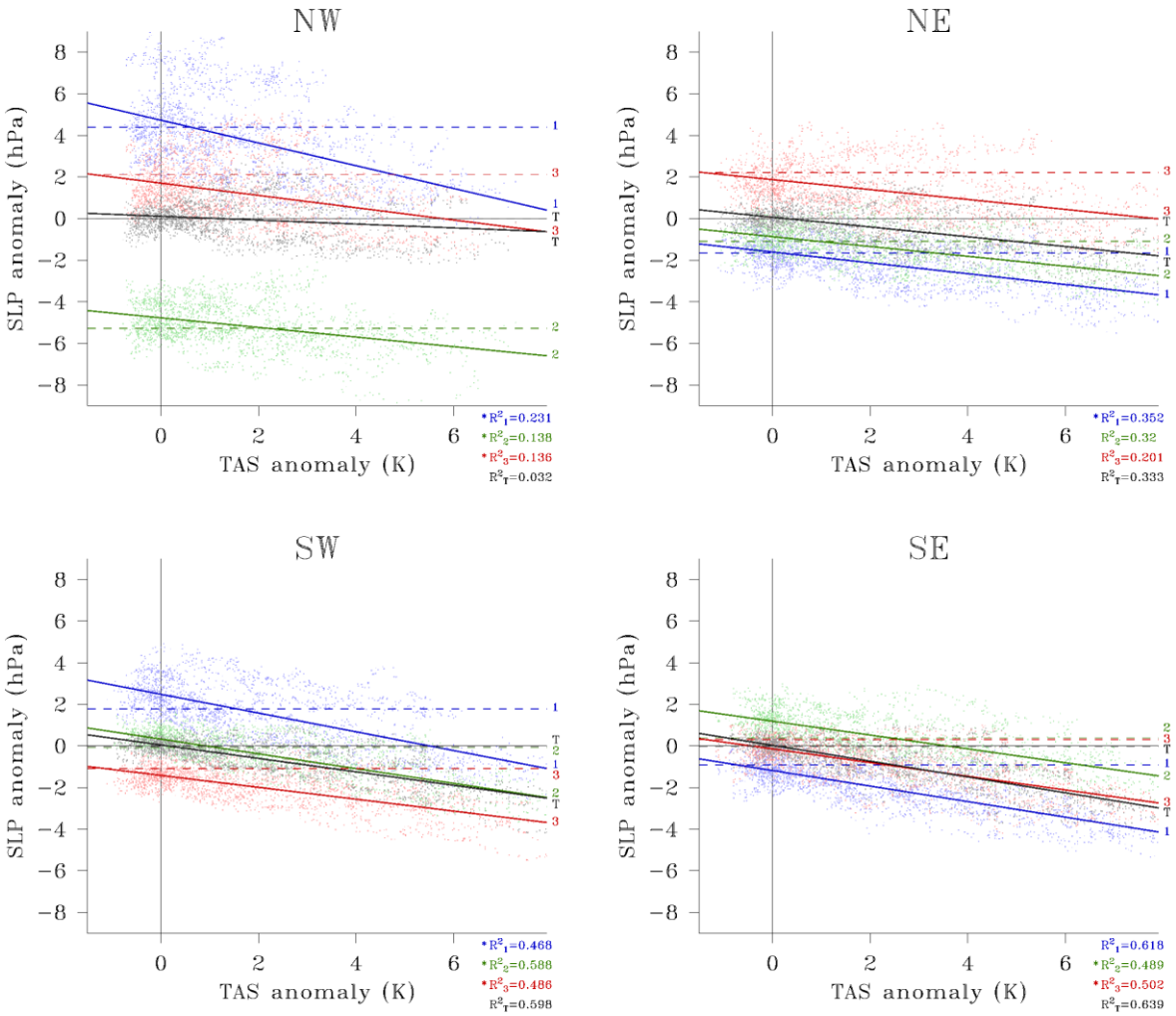

Figure 7: The dots represent the yearly GCM SLP anomaly (with regard to the JJA 1960-1999 mean and after a 10-year running mean) as a function of the total (i.e. over all Types) TAS change with regard to the JJA 1960-1999 mean using the Historical experiment (1951-2005) and the future projection RCP8.5 experiment (2006-2100). A linear regression line for the CMIP5 ensemble mean is plotted for each type (1, 2, and 3) and the total yearly mean (T) (see the determination coefficients). (*) indicates that the slope is significantly different from the (black) total slope following a Student t-test at a 5 % confidence level. The ERA-40 reference SLP anomalies (JJA, 1960-1999) are represented by the dashed lines.

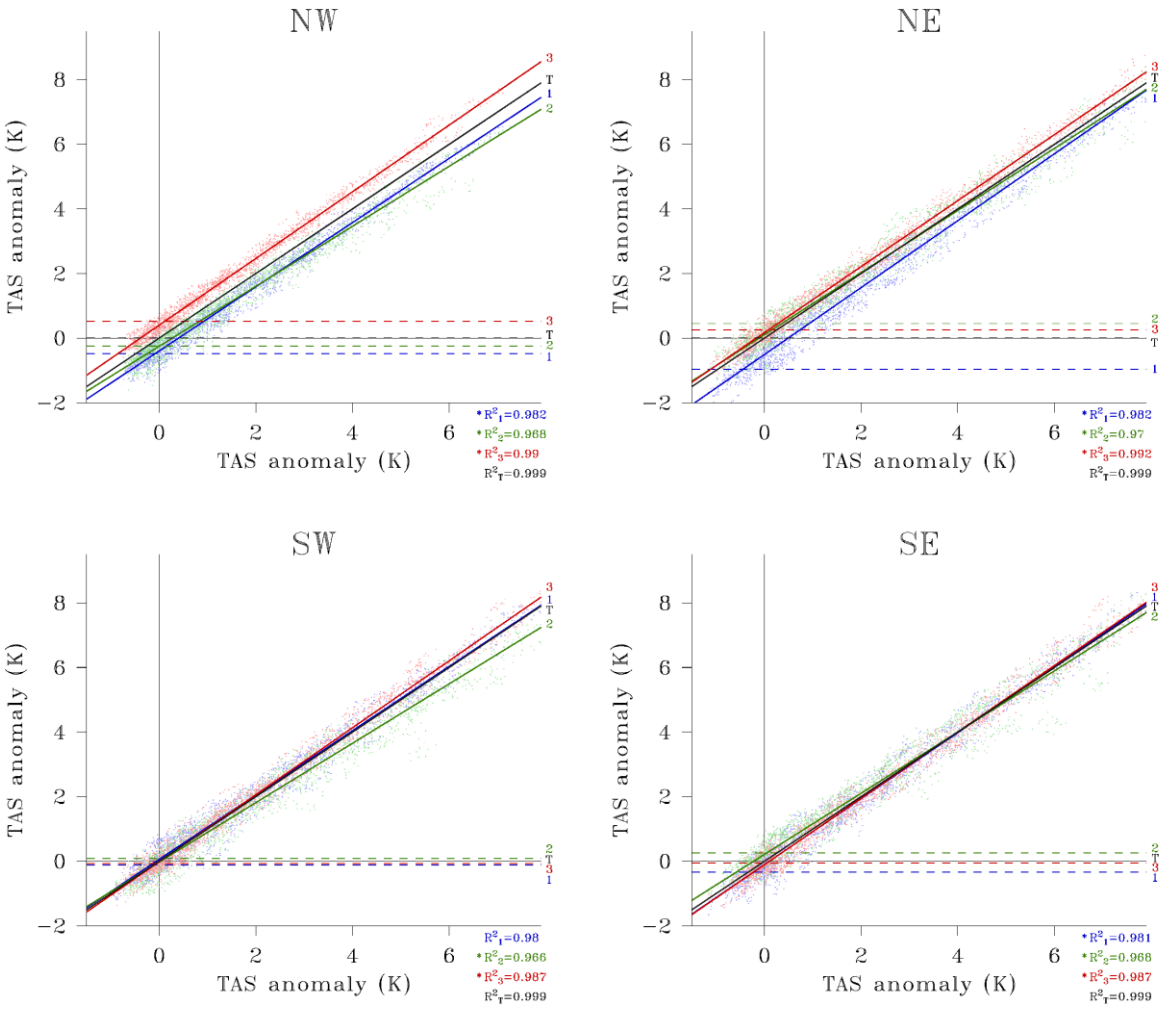

Figure 8: The dots represent the yearly GCM TAS anomaly (with regard to the JJA 1960-1999 mean and after a 10-year running mean) as a function of the total (i.e. over all Types) TAS change with regard to the JJA 1960-1999 mean using the Historical experiment (1951-2005) and the future projection RCP8.5 experiment (2006-2100). A linear regression line for the CMIP5 ensemble mean is plotted for each type (1, 2, and 3) and the total yearly mean (T) (see the determination coefficients). (*) indicates that the slope is significantly different from the (black) total slope following a Student t-test at a 5 % confidence level. The ERA-40 reference TAS anomalies (JJA, 1960-1999) are represented by the dashed lines.